Available online at www.sciencedirect.com

ScienceDirect

Acta Materialia 83 (2015) 227–238

Acta MATERIALIA

www.elsevier.com/locate/actamat

Incompatibility stresses at grain boundaries in Ni bicrystalline micropillars analyzed by an anisotropic model and slip activity

I. Tiba,[a,b,*] T. Richeton,[a] C. Motz,[b] H. Vehoff[b] and S. Berbenni[a]

[a]*Laboratoire d'Etude des Microstructures et de Mécanique des Matériaux (LEM3), UMR CNRS 7239, Université de Lorraine, Ile du Saulcy, 57045 Metz, France*

[b]*Chair of Experimental Methods in Materials Science, Saarland University, D-66041 Saarbrücken, Germany*

Received 19 June 2014; revised 15 September 2014; accepted 16 September 2014

Abstract—Incompatibility stresses can develop in bicrystals due to material elastic and plastic anisotropies owing to different crystal orientations separated by grain boundaries. Here, these stresses are investigated by combining experimental and theoretical studies on 10 μm diameter Ni bicrystalline micropillars. Throughout stepwise compression tests, slip traces are analyzed by scanning electron microscopy to identify the active slip planes and directions in both crystals. An analytical model is presented accounting for the effects of heterogeneous elasticity coupled to heterogeneous plasticity on the internal mechanical fields. This model provides explicit expressions of stresses in both crystals considering experimentally observed non-equal crystal volume fractions and inclined grain boundaries. It is used to predict the resolved shear stresses on the possible slip systems in each crystal. The predictions of the onset of plasticity as given by the present model in pure elasticity are compared with those given by the classical Schmid's law. In contrast with Schmid's law, the predictions of the analytical model are in full agreement with the experimental observations regarding the most highly stressed crystal and active slip systems. The effects of plastic incompatibilities are also considered in addition to the elastic ones throughout the model. The analysis shows that elastic/plastic coupling incompatibilities together with different crystal volume fractions have significant effects on the slip system activation process.

Keywords: Internal stresses; Anisotropic elasticity; Grain boundaries; Micropillars; Slip-lines

1. Introduction

Many recent studies, both experimental and theoretical, have investigated the mechanical behaviors of single-crystalline micropillars (SCMPs) [1–16] and bicrystalline micropillars (BCMPs) [17–21]. These studies were mainly focused on size effects on the stress–strain response. A "smaller is stronger" hardening effect was associated with a decrease in micropillar diameter [8–12,19]. Spatial–temporal slip intermittency was also studied by analyzing stress and strain drop distributions in SCMPs [11–16].

In the case of BCMPs, incompatible stresses develop in the course of mechanical loading due to grain boundaries (GBs) [22,23]. These incompatibility stresses add to the applied stress and may be responsible for the early initiation of slip bands, which can in turn trigger cracks [24]. Thus, BCMPs are good candidates to compare the theoretical predictions of the activation of slip systems at GBs to the experimental observations. First of all, the amount of slip activity can be predicted by the calculation of elastic and plastic incompatibility stresses which directly affect the resolved shear stress (RSS) values. Second, the slip system activation process may also depend on the dislocation transmission phenomena occurring at GBs [25–29].

A few years ago, important analytical studies [30–32] were carried out to compute the elastic incompatibility stresses in the general context of heterogeneous anisotropic elasticity with small plastic deformations where the bicrystal is composed of two half spaces. This solution was obtained implicitly and was checked by the finite-element method (FEM) regarding stress fields of finite bicrystals to be approximately valid in the neighborhood of GBs [33]. Recently, this solution was retrieved and explicitly derived using field dislocation mechanics theory [34]. It was also observed that analytical explicit solutions perfectly match the FEM results for the same boundary value problem [34]. In the previous approaches, the stress field was considered only for the case where the crystal volume fractions are equal [31,32,34]. To the authors' knowledge, none of these studies considered the full coupling between elastic and plastic incompatibilities with different crystal volume fractions.

In the present paper, the explicit analytical formula will be derived and applied to nickel BCMPs taking into

* Corresponding author at: Laboratoire d'Etude des Microstructures et de Mécanique des Matériaux (LEM3), UMR CNRS 7239, Université de Lorraine, Ile du Saulcy, 57045 Metz, France. Tel.: +33 87 54 73 81; fax: +33 3 87 31 53 66.; e-mail: Idriss.tiba@univ-lorraine.fr

http://dx.doi.org/10.1016/j.actamat.2014.09.033

1359-6462/

consideration the crystal volume fraction, GB inclination and full anisotropic elasticity/plasticity all together. In Section 2, the mechanical testing of Ni BCMP is introduced. In Section 3, the stress–strain curves and the slip trace analysis are reported. Then, the theory is presented in Section 4. In Section 5, the predictions of the model are discussed in the light of experimental observations and slip transfer parameters.

2. Setup of the Ni BCMPs

2.1. Material preparation

High-purity Ni was investigated (99.99%). Ni has a relatively high elastic anisotropy factor with $A = 2.37\left(A = \frac{2C_{44}}{C_{11}-C_{12}}\right)$. It also presents the advantage of easy observation of slip lines [22,35]. Specimen plates 2 mm thick were heat treated at different temperatures ranging from 1200 to 1400 °C for ~3 days in order to produce a fully recrystallized microstructure with a maximum grain size of 5 mm and GBs more or less normal to the top surface. After each annealing step, the samples were ground, mechanically polished with up to 4000 SiC paper and then finally polished with diamond abrasives down to 0.25 μm. The specimens were then electropolished in order to obtain a perfectly clean surface. Local orientation of the electropolished sample surface was characterized by electron backscattering diffraction (EBSD) performed in a Carl Zeiss ΣIGMA series scanning electron microscope with an acceleration voltage of 20 kV. The angular resolution of the EBSD orientation measurements and the lattice orientation variation within the crystals produces a maximal variation of ±1° in the measurements of the Euler angles. The data processing was performed by Flamenco Channel 5 software (HKL Technology) with an indexing rate of ~99%. The microstructure of the sample was presented by both inverse pole figure (IPF) maps and image quality (IQ) maps.

2.2. Micropillar fabrication processes

The present study focuses only on bicrystals with GBs nearly parallel to the loading direction and with expected high incompatibility stresses. Hence, the numerous Σ3 ⟨1 1 1⟩ twin boundaries (TBs) which developed under the heat treatment [36–39] were not considered since, as reported in Refs. [40,41], no elastic incompatibility stresses develop when TBs are parallel to the loading axis. The chosen crystallographic orientations of both crystals forming the BCMPs are presented in Fig. 1a. These two adjacent grains (CI and CII) have a misorientation angle of 55.1°, which corresponds to a large random angle GB.

Three BCMPs of cylindrical shape were milled along the selected GB using a Strata dual-beam 235 (FEI) focused ion beam (FIB). A 30 kV Ga^+ ion beam was used with a consecutive series of decreasing currents from 20 nA (coarse milling) to 0.05 nA (fine milling). This milling procedure can create slightly tapered BCMPs. The tapering angles for these BCMPs were calculated and were between 2.6° and 3.7°. In addition, the cutting procedure can produce a step at the GB due to different crystallographic orientations of the two grains [42]. The BCMPs have measured diameter at mid-height of ~10 μm and an average height of ~20 μm, which leads to a diameter to length ratio of ~2. It is worth noting that a variation in the GB plane inclination angle from the loading direction was observed for the three BCMPs: $\alpha^t = 13°$ (BCMP-1), $\alpha^t = 12°$ (BCMP-2) and $\alpha^t = 7°$ (BCMP-3). These values are given without tilt correction. The corrected values are, respectively, $\alpha^R = 10°$, $\alpha^R = 9°$ and $\alpha^R = 4°$ using $\alpha^{R,t} = 90° - \theta^{R,t}$ with a tilt angle of 52° as follows:

$$\theta^R = \tan^{-1}\left(\frac{\tan(\theta^t)}{\sin 52°}\right). \quad (1)$$

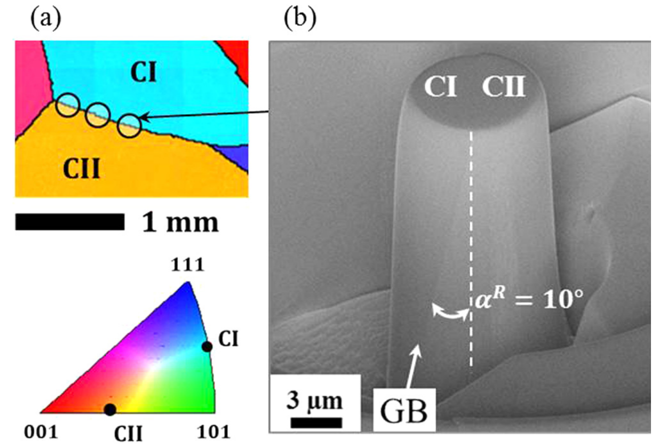

Fig. 1. (a) Inverse pole figure (IPF) map of the local grain structure constituted of two components: crystal I (CI) and crystal II (CII). The crystallographic orientation of each crystal is given in the standard triangle for face-centered cubic materials indicating the normal direction to the map. (b) SEM image of the machined BCMP and GB location after FIB milling.

Fig. 1b shows a scanning electron microscopy (SEM) image of the BCMP-1 used for compression tests taken from a view at a tilt of 52°.

2.3. Micromechanical testing

Uniaxial compression tests were performed on the three BCMPs by using a flat punch diamond indenter tip with a 20 μm end diameter connected to a Triboindenter (Hysitron) nanoindentation system. The tests were performed in displacement-controlled mode at room temperature with a displacement rate of 1 nm s^{-1}. The tests were interrupted at prescribed strains: 1.5%, 3% and 4.5% for BCMP-1, 1.5%, 3% and 6% for BCMP-2, and 1.5%, 3% and 9% for BCMP-3. Their engineering stress–strain curves were then calculated. The specimens were unloaded at these strains in order to investigate the emerged slip lines. The engineering stress was obtained by dividing the applied load by the BCMP cross-section at mid-height. The engineering strain was calculated as the displacement divided by the initial BCMP average height (~20 μm).

3. Experimental results

The three BCMPs tested showed similar deformation features and therefore, for brevity, only the results from one BCMP (BCMP-1) are presented and analyzed in detail. In the following, BCMP will refer to BCMP-1 for simplicity.